11th Australasian Fluid Mechanics Conference
University of Tasmania, Hobart, Australia
14-18 December 1992

INVESTIGATION OF SEPARATION BUBBLES AND INCLINED EDGE VORTICES ABOVE MODEL BUILDINGS USING LASER DOPPLER ANEMOMETRY

A.J. MINSON and C.J. WOOD

Department of Engineering Science, University of Oxford
Parks Road, Oxford OX1 3PJ, UNITED KINGDOM

1.0 INTRODUCTION

The Laser Doppler Anemometer (LDA) is well suited to the investigation of flow around buildings because, unlike the hot-wire anemometer, it can isolate any individual instantaneous velocity component. This remains true in the highly turbulent, reversing flows that arise in the natural wind, and the LDA is equally effective in separation bubbles and vortices.

This paper describes some separated flow and vortex measurements currently in progress in the Oxford University environmental wind tunnel. A simple cube model, placed with a roof edge normal to the incident flow, produces separation over part of the flat roof. Rotating the wind azimuth then inclines this leading edge and changes the separation pattern into a conical inclined edge vortex. This range of flows is being examined systematically using a Dantec two-component back scatter LDA with a fibre-optic link to a remote probe mounted on a traversing robot.

Interest in separated flows above buildings arises because of the large suctions that occur beneath them, and the need to represent them correctly in mathematical models. In 1977 Aroussi and Ferris used LDA to study mean velocities in the flow around model rectangular buildings, but until now there have been no velocity measurements specifically in the separation regions adjacent to roof edges. In the Oxford experiments, these flow patterns are being examined in detail for the first time, and this paper presents a preliminary view of some of the characteristics that have been observed.

2.0 EXPERIMENTAL FACILITIES AND ANALYSIS TECHNIQUES

2.1 Wind Tunnel

In the 4m by 2m wind tunnel at the University of Oxford [8] different atmospheric boundary layers can be modelled by varying the configuration of a grid at the inlet and by changing roughness elements in the 12m flow development length upstream of the turntable. A computer controlled robot is used to position probes above the turntable with an accuracy of ±0.2mm vertically and ±1mm in each horizontal direction.

2.2 Laser Doppler Anemometer

Details of the LDA system are presented in Table 1. The source is a 300mW argon-ion laser, connected by a short fibre optics link to the transmitter, which includes a Bragg cell. The four split beams for the two measurement components then pass along a further 5m fibre-optic cable to the probe and are focussed to intersect in a common measuring volume 46.3mm from the probe. The back-scattered light is returned in the same cable by a fifth fibre.

To produce adequate seeding, two aerosol generators (Thermo-Systems Inc.) are placed among the roughness elements approximately 3m upstream of the model. The particles disperse quickly in the high turbulence and are well distributed by the time they reach the measurement area. A glycerine water mixture is used as a non-toxic aerosol and from the manufacturers results on similar materials, the largest size particle is estimated to be approximately 4μm. It can be shown that such particles follow a 100Hz sinusoidally fluctuating flow with greater than 99% accuracy.

To process the photomultiplier outputs for the two components, the system includes two Dantec Burst Spectrum Analysers. These determine frequency within each signal burst using a discrete Fourier transform, and the frequency is then used to compute the instantaneous velocity of the particle causing the signal burst. Bursts are validated as relating to single particles, by requiring that the peak Doppler frequency must be greater than four times other maxima in the spectrum. Non validated bursts, which might lead to corrupt velocity values are rejected. The maximum data rate and

Table 1 LDA Specifications

LASER/OPTICS		
Type	Argon-ion	
Power	300mW	
Bragg Cell Freq.	40MHz	
Beams Transmitted	488.0nm	
	488.0nm Bragg Cell shifted	
	514.5nm	
	514.5nm Bragg Cell shifted	
PROBE		
Type	Back-Scatter	
Length	105mm	
Diameter	14mm	
Focal Length	50mm	
Beam Separation	8mm	
Receiving Aperture	11mm	
MEASURING VOLUME		
Beam wavelength	488.0nm	514.5nm
length	1.44mm	1.52mm
width	0.115mm	0.122mm
no.of fringes	37	37
SEEDING		
Generator type	TSI Model 9306 Atomiser	
Material	Water/Glycerine Ratio 5:1	
Mean Aero. Diameter	Approx. 1um	
PROCESSORS		
Type	Burst Spectrum Analyser	
Manufacturer/Model	Dantec 57N14	
Peak Data Rate	1.5MHz	
Capacity	16384 bursts	

overall capacity of the BSA was well in excess of the arrival frequency of seeding particles in the measuring volume.

When using the system, care was taken to set a Fourier transform frequency range broad enough to include both the highest and the lowest extreme velocities expected in the turbulent flow.

2.3 Calculation of Velocity Statistics from L.D.A. Output

The output from the LDA is a list of instantaneous values and occurrence times for the designated velocity component. For any given seeding density, the time interval between measurement bursts is likely to be small when the velocity is high and large when the velocity is low. Thus the LDA output list will include a disproportionately large number of high values, so that simple ensemble averaging always over-estimates the time-average.

A true time-average is based of course, upon the integral of the smooth curve through the randomly timed data points. As an approximation to this integral, valid for high data rates, the present numerical procedure simply includes each instantaneous velocity as a constant value throughout the time interval until the next sample. (This is known as 'time interval weighting' or 'sample and hold'.) The error in this approximation is of opposite sign to the gradient of the curve, so the gross effects should cancel for any periodic signal. The overall error in mean values has not been quantified here. The problem of weighting is considered in detail in reference 2.

3.0 EXPERIMENT DETAILS

3.1 Incident Flows

The purpose of the experiment was to observe the effect on normal edge separation bubbles and inclined edge separation vortices, of changes in the structure of the incident wind - particularly the intensity and frequency of the turbulence. Using suitable roughness elements and grid arrangements in the upstream part of the tunnel, four different flows were set up over the empty turntable. The flow characteristics were measured with a vertically aligned hot wire anemometer, above the turntable centre.

The mean longitudinal velocity (U) profiles were similar up to roof level (h) (figure 1), but the turbulence intensities increased from 20% at roof level (Flow No.4) to 28% at roof level (Flow No.1). The complete turbulence intensity profiles are shown in figure 2.

Longitudinal gust frequency spectra at roof height are shown in figure 3.

3.2 Model Cube

The experiments were conducted on a cube of side 200mm (i.e. h=200mm). In order to define a sharp machined corner on the separation edge, both the windward vertical face and the top were made of perspex with surface roughness of 2μm. In all four incident flows, the Reynolds number based on h and the mean undisturbed wind speed at roof height (Uh) was approximately 10^5.

3.3 Measurements with the Laser Doppler Anemometer

LDA Measurements were made with the wind direction normal to the separation edge and also at an angle of 45°. The velocity components sought were the vertical component (W) and the local horizontal component at right angles to the separation edge (Ul). Thus in both cases the plane of the measured velocity components was normal to the separation edge of the cube and approximately normal to the principal vorticity vector in the recirculating flow.

The grid of measurement locations was defined in a plane which was also normal to the separation edge of the cube. For each of the four incident flows, the measurement plane was located at the mid-point of that edge. In addition, for flow No.2 and the 45° wind azimuth only, the measurements were repeated on planes at the quarter points of the separation edge.

Measurements at each location were conducted for 120s with valid data rates between 50 Hz and 100Hz.

To measure the desired components, it was necessary to

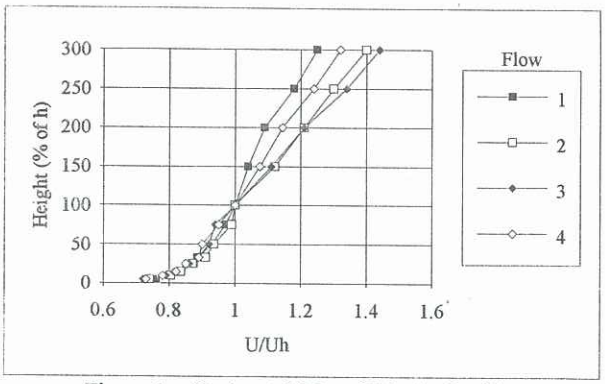

Figure 1 Horizontal Mean Velocity Profiles

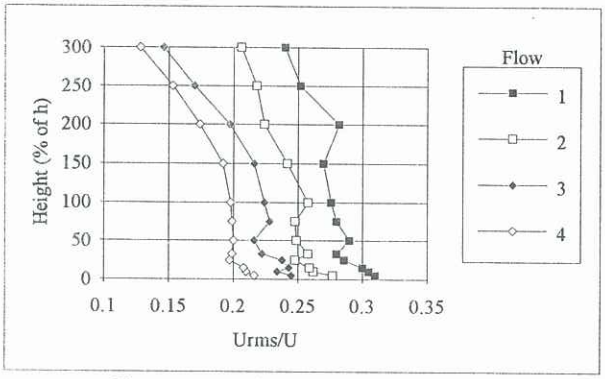

Figure 2 Turbulence Intensity Profiles

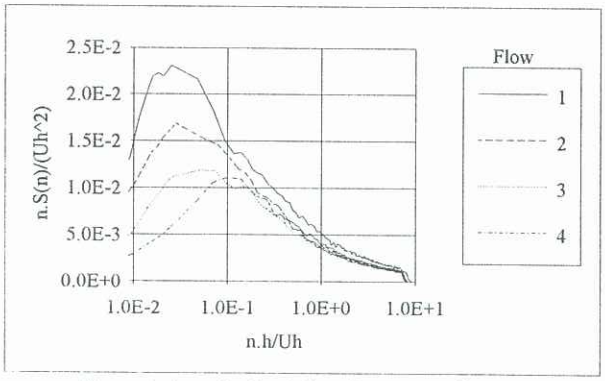

Figure 3 Longitudinal Gust Frequency Spectra
(n=measured frequency, S(n)=spectral density at n)

align the probe axis parallel with the separation edge of the cube. However the 14 mm diameter probe body then touched the cube while the measurement volume was still 7mm from the surface. When measuring closer than this, the probe was inclined by up to 9.5°. The measurement of the horizontal component (Ul) was unaffected by this rotation, but at 9.5° inclination, the second measured component W* corresponded to 0.986W - 0.165V where V is the component parallel to the separation edge and towards the probe. The correction for a 9.5° inclination is:

$$W = (W^* + 0.165\,V) / 0.986 \qquad [1]$$

In the case of the normal edge separation bubbles, V was negligible and the inclination small, so any correction was insignificant. However for the inclined edge separation vortices, V was an order of magnitude greater than W. To correct the misalignment error under these conditions, the probe was rotated through 90°, V was measured separately and then equation 1 was applied.

4.0 RESULTS

In this section, a selection of results are presented in order to highlight some of the more interesting observations that have arisen so far in the current research program. The velocities are expressed as ratios with the mean undisturbed wind speed at roof height (Uh).

4.1 Normal Edge Separation Bubbles

Figure 4 shows the locus of zero mean horizontal velocity Ul. To draw this isotach diagram, linear interpolation was used between points on the measurement grid.

The probability distributions in figure 5 illustrate, for flow No.2 how the turbulence changes with height and distance from the leading edge. Each histogram is an approximation to a conventional probability distribution. Values plotted are percentage times associated with each velocity interval, and are obtained by summing the time intervals following the velocity samples falling within each velocity range.

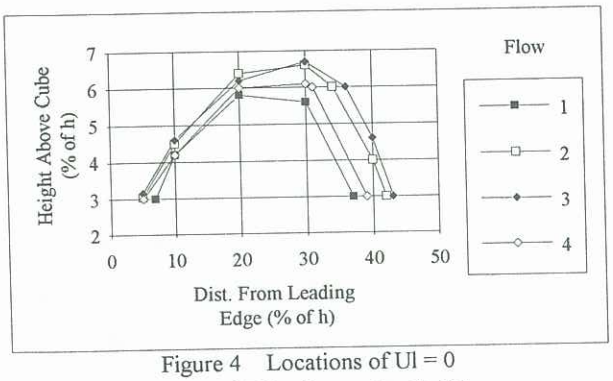

Figure 4 Locations of Ul = 0 in Normal Edge Separation Bubble

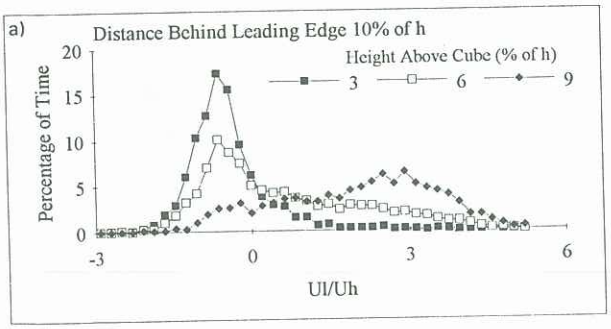

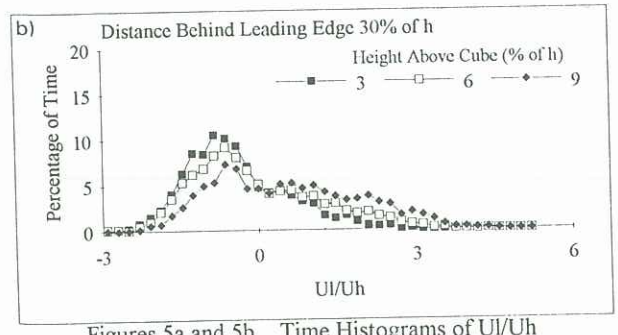

Figures 5a and 5b Time Histograms of Ul/Uh in Normal Edge Separation Bubble in Flow No.2

4.2 Inclined Edge Separation Vortices

For the particular case of incident flow No.2, the inclined edge separation vortex was examined not only in the centre-edge plane, but also in parallel planes at the quarter points. In figure 6, the vector plots in each of these three planes are presented.

5.0 DISCUSSION AND CONCLUSIONS

5.1 Normal Edge Separation Bubbles (Figures 4 & 5)

It is accepted that the effect of increased turbulence intensity, in particular small scale turbulence, is to reduce the size of separation regions (Laneville et al (1975)).

Considering just the turbulence intensity, the flows examined here may be ordered 4,3,2,1 (figure 2) whereas the order based upon decreasing size of separation bubble (figure 4) is 3,2,4,1. Clearly flows 1,2 and 3 obey the expected trend but flow 4 is out of order.

Examining the frequency spectra for these flows, it is apparent that while the spectra for the flows 1,2 and 3 peak at a similar frequency, flow 4 peaks at a higher frequency. This encourages the idea that the dominant effect on bubble size is indeed the high frequency elements in the turbulence.

To isolate high frequency turbulence quantitatively, it may be appropriate to compare, not the whole area under the spectrum, but rather the area above a selected frequency. Vickery (7) defines this by the integral

$$\left[\int_{N}^{\infty} S(n)\, d(n)\right]^{0.5} / U \qquad [2]$$

where N is a limiting frequency. Taking areas in figure 3 above an arbitrary frequency 0.1, the flows may be ordered 3,4,2,1. Compare this again with the decreasing size order of the separation bubble, 3,2,4,1, and flow 4 is still out of order but less severely so.

Further conjecture at this stage, is pointless because up until now the mean velocity profiles have been assumed to be the same for all flows, whereas above roof height there are differences. These differences in mean velocities will probably have some effect on the size of separation bubbles. Unfortunately the results are inconclusive - further work being required to isolate the effect of frequency alone. Once this is achieved the usefulness of Vickery's integral can be found. The parameter may replace the need to use both turbulence intensity and the gust frequency spectra.

The time histograms of figure 5, indicate that even 0.1h from the leading edge and 0.09h above the cube, where the mean Ul is 0.79Uh, the flow, for some periods, is reversed. The converse is true for locations where the mean Ul is negative, but instantaneously Ul can be positive and large in magnitude. It would be of interest to see the correlation between these instantaneous velocities and the surface pressures beneath. The purpose of such investigations would be to add to the work of Saathoff (1988), as reported in Melbourne (1989), who used high speed photography to investigate 'the generation, stretching and convection of vortices under the reattaching shear layer'.

5.2 Inclined Edge Separation Vortices (Figure 6)

It was expected that the effect of the incident flows on size of separation region for inclined edge separation vortices, would be the same, though less pronounced, as for normal edge separation bubbles (Kramer and Gerhardt (1991)). Although not shown here, isotach diagrams for inclined edge vortices, did show the same order of separation size according to flow No. as found for normal edge separation bubbles (figure 4). The differences between flows were less pronounced as expected. The results indicate the consistency of measurements, and in particular that the small normal edge separation region in flow No. 4, despite small turbulence intensity, cannot be dismissed as experimental error.

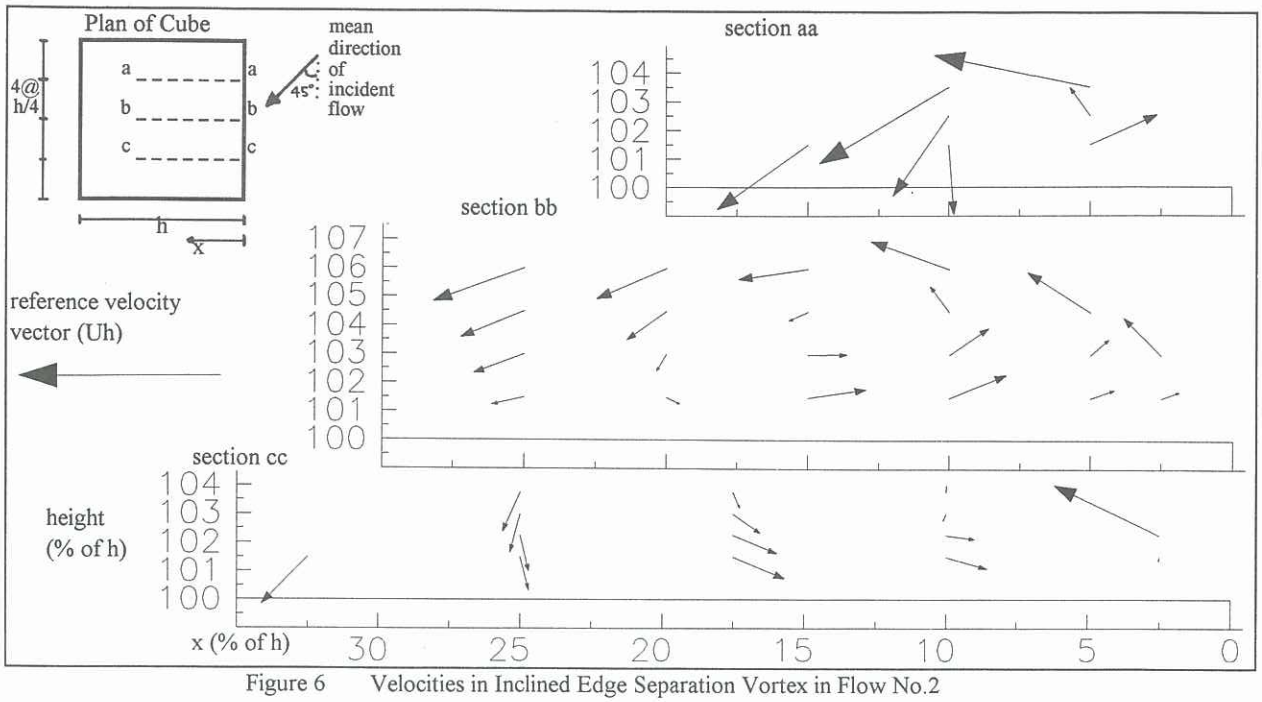

Figure 6 Velocities in Inclined Edge Separation Vortex in Flow No.2

The vector plots (figure 6) of velocities in an inclined edge vortex in flow No.2, show the increase in width and height of the vortex with increasing distance downstream. The plots also indicate that the mean velocities in the conical vortex are larger closer to the cone apex. This would be in agreement with surface pressure results that indicate greater suction nearer the cone apex. There is much scope for further investigation of inclined edge vortices at different distances downstream and it is intended to use the present facility to do this work.

The flat shape of the vortex cross-section was a surprise. Preliminary flow visualization with smoke had shown a vortex that was more circular in cross-section than the elliptical shape indicated in the vector plots. However, the visualization did also indicate that the conical vortex was intermittently swept away, leaving no identifiable flow structure until another vortex developed. The average of the flows with and without the conical vortex, would be a flatter vortex than the conical vortex seen with the smoke. The vector plots represent such an average condition and are significantly different from a representation of the instantaneous shape of a conical vortex.

It is of note that the counter rotating vortex close to the leading edge, identified by Kramer and Gerhardt (1991) with their surface flow visualization has not been identified with the LDA above a relatively shorter and taller model.

6.0 REFERENCES

1) Aroussi A. and Ferris S.A. (1987) Air Flow over Buildings: A Computer Simulation of LDA Measurements. Second Int. Conf. on Laser Anemometry - Advances and Applications, 175-188

2) Edwards R.V. (1987) Report of the Special Panel on Statistical Particle Bias Problems in Laser Anemometry. Journal of Fluids Engineering, 109 89-93

3) Kramer C. and Gerhardt H.J. (1991) Wind Pressures on Roofs of Very Low and Very Large Industrial Buildings. JWEIA, 38, 285-295

4) Laneville A., Gartshore I.S., Parkinson G.V. (1975) An Explanation of some Effects of Turbulence on Bluff Bodies. Proc. of the 4th Int. Conference on Wind Effects on Buildings and Structures, Ed. Eaton K, Cambridge University Press, Cambridge, 333-341

5) Melbourne W.H. (1989) Bluff Body Aerodynamics Review Lecture Recent Advances in Wind Engineering, Proc. 2nd Asia Pacific Symposium, Beijing China, 1, 65-76

6) Saathoff P.J. (1988) Effects of Free Stream Turbulence on Surface Pressure Fluctuations in Separated and Reattaching Flows, Ph.D. Thesis, Monash University

7) Vickery B.J. (1990) Discussions : Fundamental Studies, JWEIA, 33, 440

8) Wood C.J. (1977) The Oxford University 4m x 2m Industrial Aerodynamics Wind Tunnel, OUEL no. 1188/77